Journal of Polymer Research (2020) 27: 269
https://doi.org/10.1007/s10965-020-02247-6

ORIGINAL PAPER

Fabrication of antiseptic, conductive and robust polyvinyl alcohol/chitosan composite hydrogels

ChunHui Luo[1,2] · Yufei Zhao[1,2] · Xinxin Sun[1,2] · FaLiang Luo[3]

Received: 3 November 2019 / Accepted: 10 August 2020 / Published online: 17 August 2020

Abstract

Fabricating robust and multi-functional hydrogels is of great importance and challenge. In this work, chitosan (CS) and polyvinyl alcohol (PVA) were used to design antiseptic, conductive and robust hydrogels by a two-step method. Chemical structures of gels, the degree of crystallinity, the state of water in hydrogels, as well as their microstructures were characterized via a combination of FT-IR, XRD, DSC and SEM. Segment lengths of cross-linking points were calculated from elastic rubber theory. Their mechanical properties were evaluated on the electronic testing machine. It was shown that the tensile strength and elongation at break of single PVA hydrogel were only 200 kPa and 135%, respectively, due to the heterogenous structure with pore sizes between 1.5 ~ 8.2 μm. By introducing CS into PVA matrix followed with soaking in a saturated NaCl solution, the network became homogeneous with a pore size of 0.5 ~ 1.1 μm. Moreover, free water changed to bond water, and frictions between polymer chains increased because of hydrophobic associations and entanglements of CS segments. As a result, the tensile stress and strain increased to 3800 kPa and 270%, respectively. The gel also exhibited antiseptic property, electrical conductivity and swelling-resistant properties. The strength after reaching swell equilibrium was 3400 kPa, much higher than most gels at swollen states. This gel might find applications in bionic cartilage, sensors, food preservation and wearable devices.

Keywords PVA · Chitosan · Robust · Antiseptic · Conductive

Introduction

As three-dimensional networks of polymer chains swelling in water, hydrogels were considered as one of the best candidates in drug delivery, tissue engineering, soft electronics and wound dressings, because of their structural similarities to human tissues and organs [1–4]. Conventional polyacrylamide(PAM) gels are usually fragile arose from the heterogeneity cross-linking network and low density of polymer chains [5]. Therefore, developing tough and functional gels is urgently necessary while difficult. To date, dual-network, nano composited, topological cross-linking and micellar cross-linked hydrogels were successful strategies to improve the mechanics of traditional PAM gels [6–9]. However, biocompatibility and functionalities of PAM remain a concern. Therefore, strong, biocompatible and functional gels are highly expected.

Generally, gels based on alginate, cellulose, chitosan, polyvinyl alcohol (PVA) and other biocompatible materials are safe and biocompatible [10–17]. Among them, FDA-approved PVA received much attention [18, 19]. They were usually prepared by freezing-thawing (F-T) methods and radiation cross-linking [20, 21]. However, crystalline sizes by F-T circles increase irregularly, while the network structure is uneven for the later [20], giving rise to fragile PVA gels. The gel stress from three F-T methods was reported to be less than 500 kPa [21]. Compared with tissue, these weak gels also lack conductivity and other functions, which greatly retard their

Electronic supplementary material The online version of this article (https://doi.org/10.1007/s10965-020-02247-6) contains supplementary material, which is available to authorized users.

✉ ChunHui Luo
luochunhui@iccas.ac.cn

✉ FaLiang Luo
flluo@iccas.ac.cn

[1] College of Chemistry and Chemical Engineering, North Minzu University, Yinchuan 750021, Ningxia, China

[2] Key Laboratory of Chemical Engineering and Technology, State Ethnic Affairs Commission, North Minzu University, Yinchuan 750021, Ningxia, China

[3] State Key Laboratory of High-efficiency Utilization of Coal and Green Chemical Engineering, Ningxia University, Yinchuan 750021, China

applications [22]. Consequently, fabricating robust and functional PVA gels are urgent.

To enhance gels, physical interactions including hydrogen bondings, hydrophobic associations, chain entanglements and ionic bonds were adopted, which were essential to endow gels with ability to dissipate external loads efficiently [23–26]. For example, Yang and coworkers achieved a 56-fold increase in tensile stress via coordination bonds between chitosan and sodium citrate [25]. After forming stronger hydrogen bondings between PVA and tannic acid, Jin group prepared gels with tensile strength close to 10.0 MPa [26]. Despite these achievements, their functionalities are not sufficient [26]. Another great limitation of present tough gels is that they will absorb lots of water and become fragile when immersing in water [27]. Considering the majority content of the human body is water, hydrogels with anti-swelling ability are of promising applications in tissue engineering. However, such gels are still difficult to fabricate.

Herein, synergistic physical interactions, instead of chemical cross-linkers, were adopted to achieve this goal. As a natural polysaccharide prepared by deacetylating chitin, chitosan is non-cytotoxic, pH-sensitive and antiseptic, which has shown promise as an ideal candidate for drug delivery [28–32]. It contains amine, ether and hydroxyl groups, making it possible to form H-bonds with PVA. Furthermore, its solubility was dependant on ionic strength and pH values [28], providing potential methods to induce micro-phase separation. To this end, commercially available PVA and CS were applied to design functional gels. As shown in Fig. 1, the gel was prepared by three F-T repeating followed with soaking in a 26.5 wt% NaCl solution to induce hydrophobic association of CS chains, serving as additional cross-linking points to decrease the dangling ends and loops of PVA chains. This method results in gels with exciting mechanics (strength = 3800 kPa, strain =270%, and toughness = 5900 kJ/m^3), excellent antiseptic property, electrical conductivity and anti-swelling ability, which might find application in cartilage repair, artificial skin and sensors.

Experimental section

Materials

Poly(vinyl alcohol) (PVA, M_n = 74,800 g/mol, degree of alcoholysis is 99%) and sodium chloride (NaCl, AR) were provided by Aladdin Reagent (Shanghai) Co., Ltd. Chitosan (CS, degree of deacetylation is higher than 90%, M_n = 4000 g/mol) was provided by TCI Shanghai. All agents were used without purification.

Synthesis of PVA-CS gels

The PVA-CS-X-S gel was fabricated by simple mixing and soaking. Firstly, PVA and CS powders were dissolved in hot water to form a transparent solution with the PVA mass fraction of 10%. After injecting into molds, they were put in a refrigerator (−20 °C) for 8 h and then stood at room temperature for 4 h. Through three Freezing-Thawing cycles, the PVA-CS-X gels were obtained, where X was the mass ratio of chitosan to poly (vinyl alcohol). These gels were immersed in a 26.5 wt% NaCl solution to achieve the resulted PVA-CS-X-S gels.

Characterization and instruments

FTIR analysis was carried out using the KBr method within 4000–500 cm^{-1} wavenumber (Nicolet Avatar 380 spectrometer). SEM photographs were taken by the ZEISS EVO-18 electron microscopy, and freeze-dried gels were painted with gold to enhance conductivity. DSC experiments were performed on a TA Instruments (model Q20) in the N_2

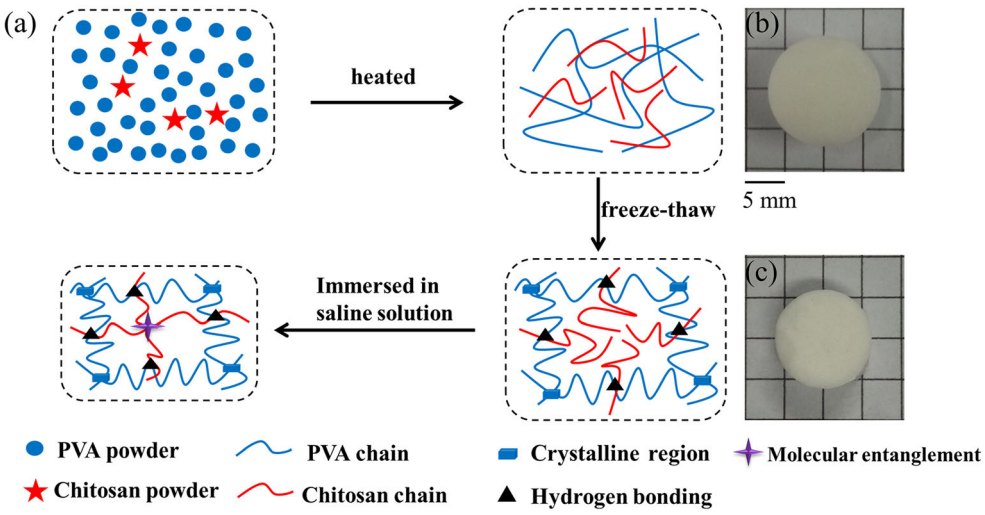

Fig. 1 **a** Synthetic mechanism of the PVA-CS-S hydrogel; transformation process of the **b** PVA-CS-5 hydrogel into **c** hybrid PVA-CS-5-S hydrogel

atmosphere from −40 °C to 40 °C for 80 min. XRD was recorded on Rigaku SmartLab X-ray diffractometer(CuKα radiation) from 5° to 80° (2θ) at a scan rate of 5 (°) / min. Water contents (X_n) were estimated by the Eq. (1) [33]:

$$X_n = \frac{Q_{endo}}{Q_f} \times 100\% \quad (1)$$

Where Q_{endo} and Q_f are the fusion enthalpy from DSC curves and that from literature (333.5 J/g) [33].

The crystallinity of PVA (χ_c) was calculated by the Eq. (2) [34]:

$$\chi_c = \frac{A_1}{A_2} \times 100\% \quad (2)$$

Where A_1 and A_2 are integral areas in the 2θ range of 18° ~ 21° and 5° ~ 80°, respectively.

Mechanical properties

Mechanical properties of gels were recorded by a HZ-1003B electronic tensile instrument. Dumbbell-shaped gels were deformed under a tensile rate of 100 mm/min. The strength (σ_b), strain (ε), elastic modulus (E) and toughness (T) were calculated by the fracture strength, elongation at break, slope of linear range (5 ~ 10%), and integral area of tensile curves, respectively [35]. To estimate the dissipated energy (U_{hys}), samples were stretched to certain strains and then released [11].

The component content and cross-linking density of the hydrogel

Water content (W_{water}) and polymer content (W_{gel}) were estimated by Eqs. (3) and (4) [36]:

$$W_{water} = \frac{W_w - W_d}{W_w} \times 100\% \quad (3)$$

$$W_{gel} = \frac{W_G \times C_G}{W_w} \times 100\% \quad (4)$$

Where W_w, W_d, W_G and C_G are the wet weight, dry weight, polymer weight and polymer mass ratio, respectively [36].

The cross-linking density (v_0) as well as chain lengths between adjacent cross-links (M_c) were estimated by Eqs. (5) and (6) [37, 38] within the elastic range (λ = 2):

$$\sigma = v_0 kT\left(\lambda - \lambda^{-2}\right) \quad (5)$$

$$M_c = \rho N_A / v_0 \quad (6)$$

Where σ, λ, k and T are the tensile strength, tensile strain, Boltzmann constant, and Kelvin temperature, respectively.

The gel fraction (F_g) and mesh size (ξ)

The gel fraction (F_g) was investigated by a gravimetric method [39, 40]. Typically, freeze-dried samples were weighed (W_o) and immersed in DI water at RT to remove the soluble linear polymers. Then they were dried at 105 °C for 24 h and weighed again (W_i). The F_g was evaluated by Eq. (7) [39, 40]:

$$F_g = \frac{W_i}{W_0} \times 100\% \quad (7)$$

The mesh size (ξ) was estimated by Eq. (8) [41]:

$$\frac{3kT}{E} = \frac{4}{3}\pi\left(\frac{\xi}{2}\right)^3 \quad (8)$$

Where E, k and T are the elastic modulus, Boltzmann constant and Kelvin temperature, respectively.

Antiseptic property

The antiseptic properties of gels were measured by the observation method [42]. PVA and PVA-CS-5-S gels were stored into glass bakers at 25 °C under a humidity of 30–35% and covered by a film. After 15 days, two samples were taken out and their surfaces were investigated by a digital camera.

Conductivity

Sample conductivities were investigated by recording the brightness of a green LED lamp from the gel-connected circuit [42].

Result and discussion

Preparation and characterization

The gel was obtained by mixing PVA and CS powders in hot water, followed by three F-T circles and soaking in the sodium chloride aqueous solution (Fig. 1). The interpenetrating network was firstly obtained after three F-T cycles to form crystalline microdomains of PVA, with CS chains embedded in the sticky PVA matrix. They were further soaked in a saturated NaCl solution to induce the micro-phase separation of CS chains. By doing so, the cross-linking density might increase with a decrease in dangling ends and loops of polymer chains [25]. Besides, the reversible break/reformation of multiple physical interactions (hydrophobic association, crystalline region, and hydrogen bonding) was effective to dissipate energy, which was important to achieve tough gels. Gel structures were firstly confirmed by FTIR. As shown in Fig. 2, CS displayed typical absorptions at

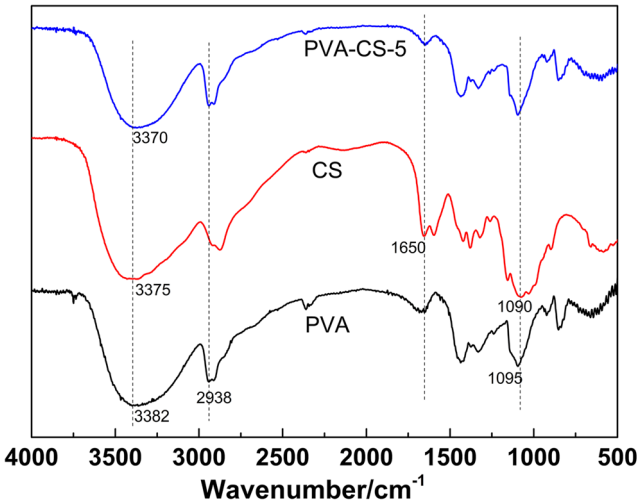

Fig. 2 FTIR spectra of PVA, CS and PVA-CS-5 gel

3375, 1650 and 1090 cm^{-1} from the vibration of N-H, C=O and C-O bonds, respectively [43]. The peaks at 3382, 2938 and 1095 cm^{-1} were associated with the vibration of O-H, C-H and C-O in PVA [44]. Peaks in PVA-CS-5 were well assigned from raw materials, while the O-H stretching at 3382 cm^{-1} decreased to 3370 cm^{-1}, suggesting that stronger hydrogen bonds were formed [45].

Mechanical performances

Mechanical performances of PVA-CS-X gels were evaluated firstly by altering CS contents. As displayed in Fig. 3, tensile strength (σ_b) and strain (ε) of single PVA gel were 200 kPa, 135%, respectively, consistent with literature reports [21]. For PVA-CS-5, the σ_b and ε reached 900 kPa and 160%, respectively. They all

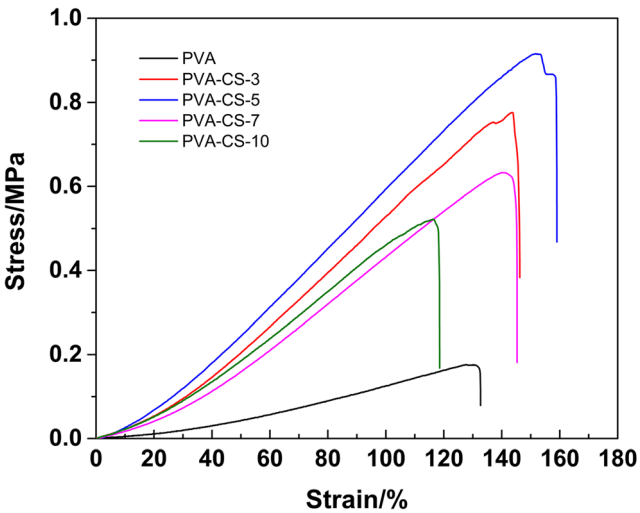

Fig. 3 Stress-strain curves of PVA-CS-X gels with various CS contents

decreased when CS contents increased to 7 wt% and 10 wt%. The cross-linking density was inadequate at lower CS contents, whereas it might be over cross-linked at higher CS contents [46]. Therefore, optimal mechanics of precursor gels were obtained for PVA-CS-5, which was further enhanced by soaking in NaCl solution to form additional joint knots.

Pioneering works revealed that the energy dissipation mechanism, cross-linking densities and network parameters were essential to fabricate tough gels [23–26]. For example, the tensile strength of a PAM/CS composite gel increased 56 times when coordination bonds were formed between cationic amino groups in CS and anionic citrate groups from solution [25]. The solubility of CS in water was also determined by pH values and ionic strength [47]. Therefore, we immersed the PVA-CS-5 precursor gels into a saturated NaCl aqueous solution to induce micro phase separation of CS. To achieve a relatively homogenous network, the soaking time was investigated firstly, and optimally mechanical properties were achieved at 50 min for the PVA-CS-5 gel. As displayed in Fig. 4a, the PVA-CS-5 gel could hold a 0.2 kg load, whereas the PVA-CS-5-S gel could bear a 2.3 kg load, indicating the soaking strategy is successful. Then we systematically investigated its mechanical performances. As illustrated in Fig. 4b, the σ_b, E and T of the resulted gel increased to 3800 kPa, 2100 kPa, 5900 kJ/m^3, which were 3.2, 8.3 and 7.2 times higher than that of the precursor gel, respectively.

To reveal the structure-property relationship and to shed light on the energy dissipation mechanism, the hysteresis test was performed [48, 49]. As displayed in Fig. 4c and d, three gels all exhibited hysteresis loops, indicating energy dissipation mechanism. However, the dissipated energy of PVA-CS-5-S (592.1 kJ/m^3) was much higher than the other two gels, suggesting that chain entanglements of CS after immersion could distribute external load efficiently. Moreover, the ratio of the dissipated energy to the total energy was 80.9%, further confirming the effective energy dissipation mechanism. To summarize, chain entanglements of CS in the sticky PVA matrix could significantly toughen the gel.

Property-structure relationship

Water states and the corresponding contents, and network parameters were also calculated via DSC, SEM, XRD and theoretical estimation. Solid contents were firstly obtained from the weighing method [36]. As shown in Fig. 5a, water content decreased from 89.1 wt% for PVA-CS-5 to 59.2 wt% for PVA-CS-5-S, accompanied by an increase in polymer contents from 10.9 wt% to 17.7 wt%. A higher polymer mass fraction would lead to a stronger

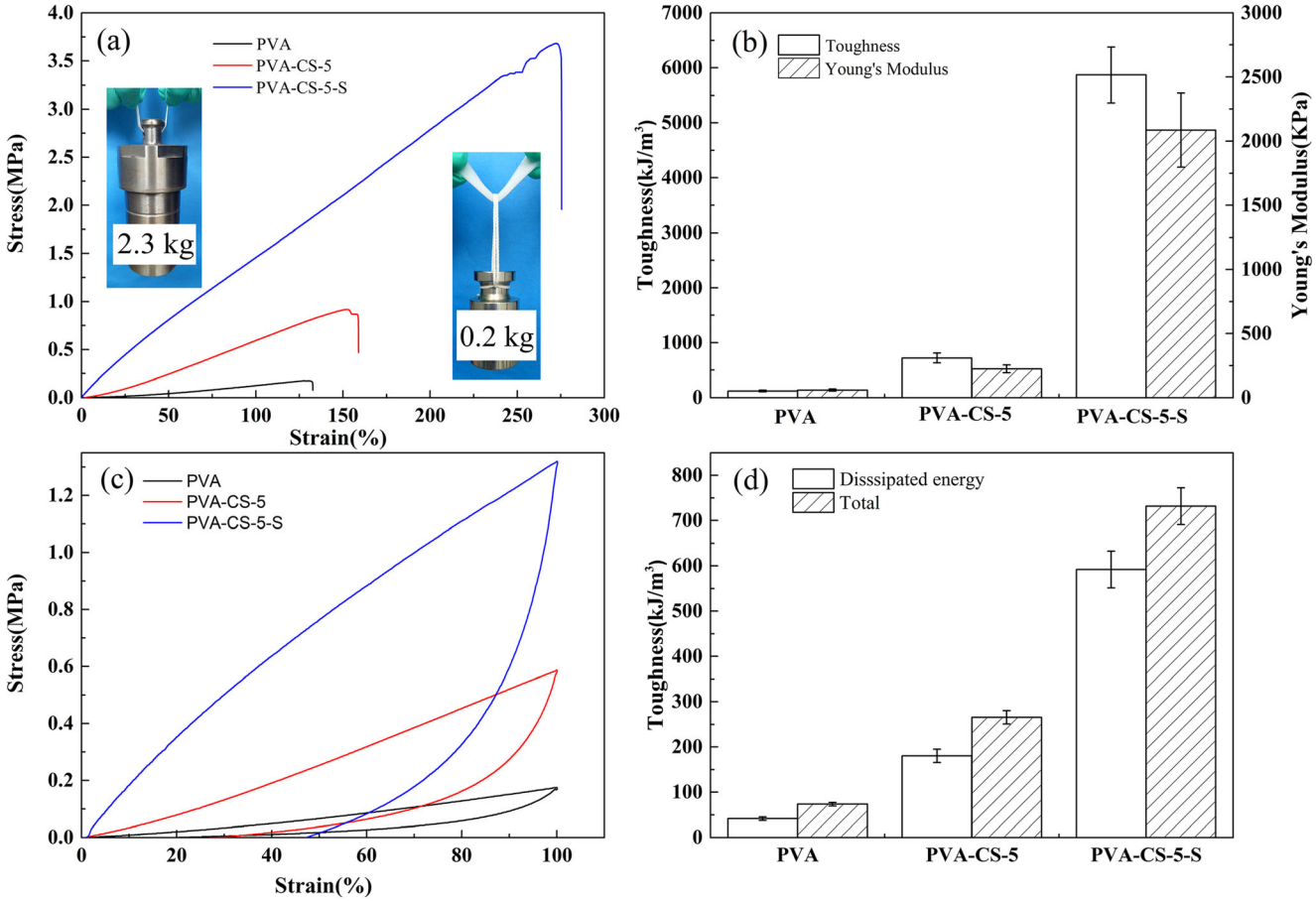

Fig. 4 **a** Stress-strain curves, **b** toughness, young's modulus, **c** the loading-unloading curves and **d** the dissipated and total toughness of three gels

gel [50]. Contents of free water (FW), freezable bound water (FBW) as well as non-freezable bound water (NBW) were also determined from DSC curves [51, 52]. As displayed in Fig. 5b, the PVA-CS-5 gel exhibited an endothermic peak from FW around 1.5 °C. Based on Eq. (1) [33], contents for FW and NBW were 62.8 wt% and 26.3 wt%, respectively. After immersion in NaCl, the endothermic peak decreased from 1.5 °C to −18.4 °C. The contents for FW, FBW and NBW were 0, 33.3 wt% and 25.9 wt%, respectively. Generally, the decline of FW content would increase internal frictions of polymers [42], resulting in better mechanical performances. The crystallinity of PVA was analyzed by XRD. As shown in Fig. 5c, both samples shown strong characteristic diffraction peaks in the 2θ range 18 ~ 21°, corresponding to the 101 crystal plane of PVA. The crystallinity of PVA reduced slightly from 14.8% to 12.3% after soaking. The effective cross-linking density (v_0) of the gel and molecular weight of cross-linking points (M_c) were also calculated from Eqs. (5) and (6). As displayed in Fig. 5d, the v_0 and M_c for the former were only 136.6 mol/m^3 and 7757 g/mol, while became 336.1 mol/m^3 and 3594 g/mol for the later. A rise in v_0 (or a decline in M_c) would result in a stronger gel [37]. In summary, free water content and crystallinity of PVA decreased while the frictions between polymer chains and cross-linking density increased after soaking in NaCl. Consequently, the gel was enhanced.

Network parameters were also revealed by SEM. As displayed in Fig. 6, they all exhibited typical spongy structures [53]. However, single PVA gel (Fig. 6a) had uneven heterogenous structures with pore sizes ranging from 1.5 to 8.2 μm. The network became denser after mixing with CS (Fig. 6b). After immersion into the saturated NaCl solution, the pore size decreased to ~1.0 μm (Fig. 6c), suggesting a densest network. To further clarify this, gel fraction (F_g) of two gels were estimated, assuming that polymers were in Gaussian distribution in the gel network [41]. The F_g for PVA-CS-5 and PVA-CS-5-S were 58.6% and 87.2%, respectively. Higher F_g indicated fewer defects (loops and dangling chains), consistent with previous calculation in Fig. 5d. Meanwhile, the mesh size of network decreased from 98 Å to 48 Å. The results indicated that the gel became more compact and uniform

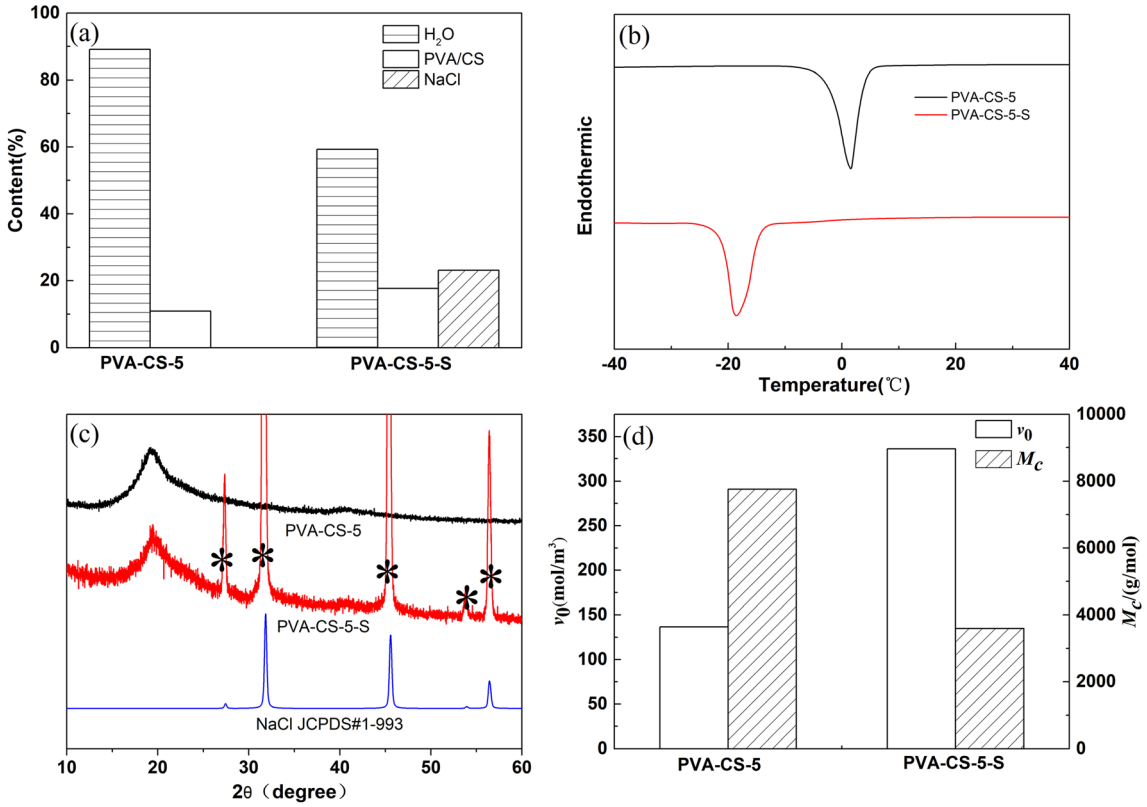

Fig. 5 **a** The mass contents of each component, **b** DSC curves, **c** XRD patterns (peaks from NaCl was marked with star); **d** v_0 and M_c of two gels upon soaking

after soaking, consistent with SEM images. Generally, a rise in gel fraction and a decline in mesh size would result in a stronger gel [41].

Considering the potential application of our gel is bone repair, and the human body is a water-rich environment, we further examined the tensile properties of PVA-CS-5-S gel when reaching a swelling equilibrium in DI water. As displayed in Fig. 7, the σ_b and ε of the swollen gel were 3400 kPa and 218%. Compared with the as-prepared gel, the retentions of stress and strain were as high as 89.5% and 80.7%, respectively, indicating good swelling-resistant ability. The mechanical properties of our gel at the swollen state are among the top values of physical gels in literature [10, 11, 23, 44]. More importantly, the stress is much higher than traditional PAM gels at swollen states. For instance, the σ_b of a traditional PAM gel was only 20 kPa [27]. The excellent anti-swelling ability was probably due to the fewer defects and even distribution of knots in the gel network [27]. Another contribution might be the multiple interactions in our system including crystallinity of PVA and hydrophobic association of CS chains, which were rather stable at room temperature and non-acidic water, respectively [20, 28, 32].

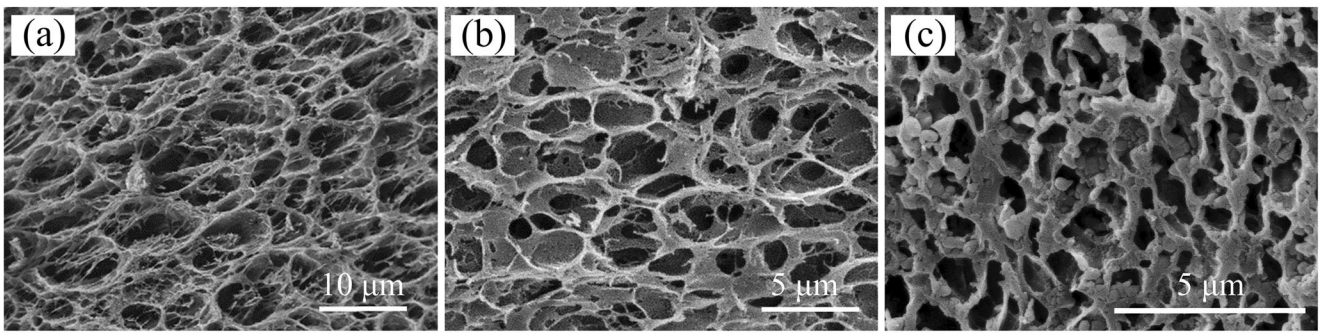

Fig. 6 SEM photographs of **a** PVA, **b** PVA-CS-5 and **c** PVA-CS-5-S gels

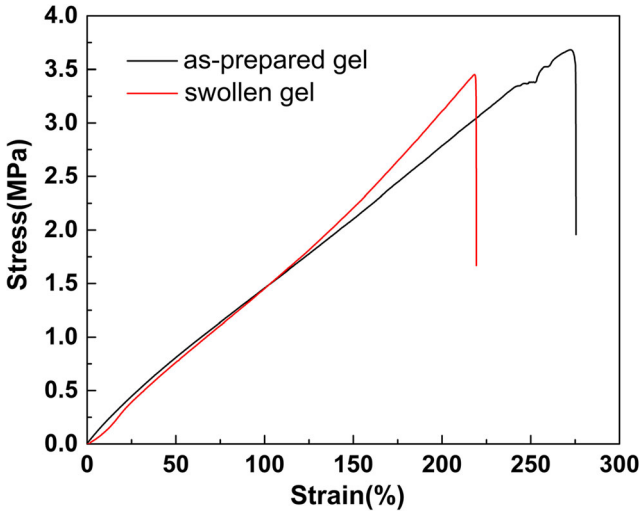

Fig. 7 Mechanical properties of the as-prepared (black) and swollen (red) PVA-CS-5-S gel

Multi-functionalities of the obtained gel

As a natural polysaccharide, chitosan was non-cytotoxic, pH-sensitive and antiseptic, which has shown promise in drug delivery for several years [28–32]. We were curious about the functions of this gel. We then investigated the antiseptic property as well as the conductivity of PVA and PVA-CS-5-S gels. As Fig. 8a displayed, after 15 days culture, obvious mold growth was observed at the surface of PVA gel, while nothing appeared on the surface of PVA-CS-5-S gel, indicating good antiseptic properties. Later, the conductivities of two samples were compared. As illustrated in Fig. 8c and d, the LED bulb was shining when PVA-CS-5-S gel was assembled in the circuit, while it was dim when PVA gel was adopted, suggesting potential applications in sensing elements and wearable devices. Furthermore, the NaCl concentration was around 0.07 mmol per adult body weight (ABW) (supposing ABW = 60 kg) [54, 55], less than 205 mmol//kg ABW, which might induce hypernatremia [56], indicating our gel maintained the biocompatibility of PVA and CS.

Conclusion

In this work, an antiseptic, conductive, swelling-resistant and robust gel was fabricated from two commercially available materials, PVA and CS. Because of the synergistic interactions including chain entanglements of CS, hydrogen bonds between PVA and CS, and crystalline domains of PVA, the resulted gels exhibited excellent mechanical performances, superior to most physical gels. Besides, it was antiseptic, conductive and swelling-resistant. The tensile strength of our gel was 3400 kPa even reaching a swelling equilibrium in water, much stronger than most water-rich gels. The robust and multi-functional material would have potential applications in tissue engineering and sensors.

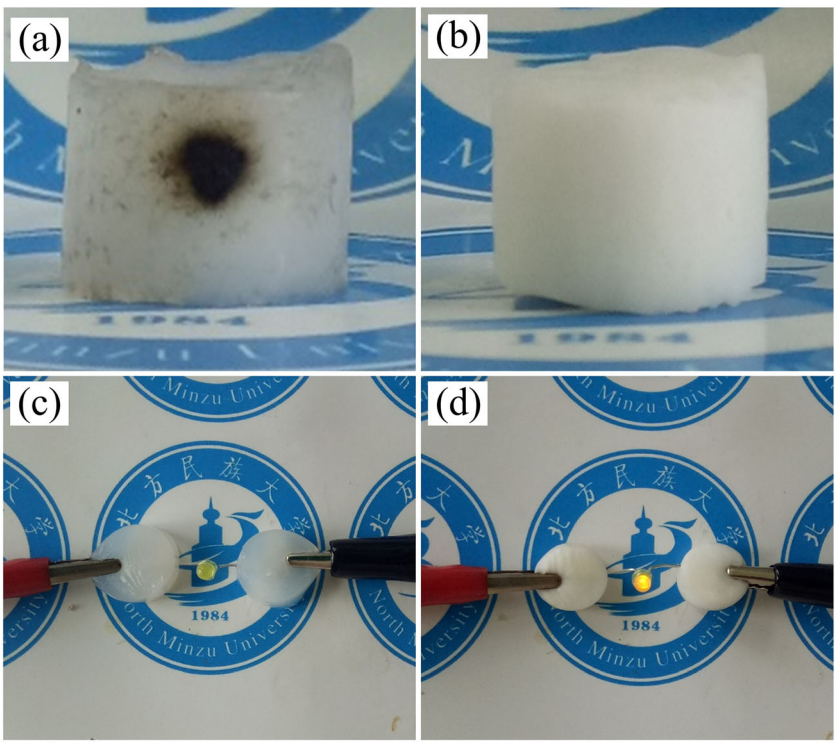

Fig. 8 The antiseptic property of **a** PVA gel and **b** PVA-CS-5-S gel, the conductive properties of **c** PVA gel and **d** PVA-CS-5-S gel

Acknowledgements This work was supported by the Specialized Research Fund in Ningxia Higher Education Institutions (NGY2018-165), Natural Science Foundation of Ningxia Province (2020AAC03205), and Natural Science Foundation of China (21464001).

Compliance with ethical standards

Competing interest The authors declare no competing financial interest.

References

1. Li J, Mo LT, Lu CH, Fu T, Yang HH, Tan WH (2016) Functional nucleic acid-based hydrogels for bioanalytical and biomedical applications. Chem Soc Rev 45(5):1410–1431
2. Thiele J, Ma Y, Bruekers SMC, Ma SH, Huck WTS (2014) 25th anniversary article: designer hydrogels for cell cultures: a materials selection guide. Adv Mater 26(1):125–148
3. Wang HY, Heilshorn SC (2015) Adaptable hydrogel networks with reversible linkages for tissue engineering. Adv Mater 27(25):3717–3736
4. An H, Chang LM, Shen JF, Zhao SH, Zhao MY, Wang XM, Qin JL (2019) Light emitting self-healable hydrogel with bio-degradability prepared form pectin and Tetraphenylethylene bearing polymer. J Polym Res 26(2):26
5. Gong JP (2010) Why are double network hydrogels so tough? Soft Matter 6(12):2583–2590
6. Gong JP, Katsuyama Y, Kurokawa T, Osada Y (2003) Double-network hydrogels with extremely high mechanical strength. Adv Mater 15(14):1155–1158
7. Haraguchi K, Takehisa T (2002) Nanocomposite hydrogels: a unique organic-inorganic network structure with extraordinary mechanical, optical, and swelling/de-swelling properties. Adv Mater 14(6):1120–1124
8. Huang T, Xu HG, Jiao KX, Zhu LP, Brown HR, Wang HL (2007) A novel hydrogel with high mechanical strength: a macromolecular microsphere composite hydrogel. Adv Mater 19(12):1622–1626
9. Okumura Y, Ito K (2001) The Polyrotaxane gel: a topological gel by figure-of-eight cross-links. Adv Mater 13(7):485–487
10. Chen F, Lu SP, Zhu L, Tang ZQ, Wang QL, Gang Q, Yang J, Sun GZ, Zhang Q, Chen Q (2019) Conductive regenerated silk fibroin-based hydrogels with integrated high mechanical performances. J Mater Chem B 7(10):1708–1715
11. Chen Q, Zhu L, Chen H, Yan HL, Huang LN, Yang J, Zheng J (2015) A novel design strategy for fully physically linked double network hydrogels with tough, fatigue resistant, and self-healing properties. Adv Funct Mater 25(10):1598–1607
12. Duan JJ, Zhang LN (2017) Robust and smart hydrogels based on natural polymers. Chin J Polym Sci 35(10):1165–1180
13. Guo FY, Wang N, Cheng QF, Hou LL, Liu JC, Yu YL, Zhao Y (2016) Low-cost coir Fiber composite with integrated strength and toughness. ACS Sustain Chem Eng 4(10):5450–5455
14. Ghasemzadeh H, Ghanaat F (2012) Antimicrobial alginate/PVA silver nanocomposite hydrogel, synthesis and characterization. J Polym Res 21(3):355
15. Sun JY, Zhao XH, Illeperuma WRK, Chaudhuri O, Oh KH, Mooney DJ, Vlassak JJ, Suo ZG (2012) Highly stretchable and tough hydrogels. Nature 489(7414):133–136
16. Yang W, Fortunati E, Bertoglio F, Owczarek JS, Bruni G, Kozanecki M, Kenny JM, Torre L, Visai L, Puglia D (2018) Polyvinyl alcohol/chitosan hydrogels with enhanced antioxidant and antibacterial properties induced by lignin nanoparticles. Carbohydr Polym 181:275–284
17. Luo CH, Sun XX, Wang F, Wei N, Luo FL (2019) Utilization of L-serinyl derivate to preparing triple stimuli-responsive hydrogels for controlled drug delivery. J Polym Res 26:280
18. Kobayashi M, Toguchida J, Oka M (2003) Preliminary study of polyvinyl alcohol-hydrogel (PVA-H) artificial meniscus. Biomaterials 24(4):639–647
19. Ghasemzadeh H, Ghanaat F (2014) Antimicrobial alginate/PVA silver nanocomposite hydrogel, synthesis and characterization. J Polym Res 21(3):355
20. Hassan CM, Peppas NA (2000) Structure and applications of poly(-vinyl alcohol) hydrogels Producd by conventional crosslinking or by freezing/thawing methods. Adv Polym Sci 153:37–65
21. Ricciardi R, D'Errico G, Auriemma F, Ducouret G, Tedeschi AM, Rosa CD, Lauprêtre F, Lafuma F (2005) Short time dynamics of solvent molecules and Supramolecular Organization of Poly (vinyl alcohol) hydrogels obtained by freeze/thaw techniques. Macromolecules 38(15):6629–6639
22. Baker MI, Walsh SP, Schwartz Z, Boyan BD (2012) A review of polyvinyl alcohol and its uses in cartilage and orthopedic applications. J Biomed Mater Res B Appl Biomater 100(5):1451–1457
23. Chen Q, Zhu L, Zhao C, Wang QM, Zheng J (2013) A robust, one-pot synthesis of highly mechanical and recoverable double network hydrogels using thermoreversible sol-gel polysaccharide. Adv Mater 25(30):4171–4176
24. Zhang HJ, Sun TL, Zhang AK, Ikura Y, Nakajima T, Nonoyama T, Kurokawa T, Ito O, Ishitobi H, Gong JP (2016) Tough physical double-network hydrogels based on Amphiphilic Triblock copolymers. Adv Mater 28(24):4884–4890
25. Yang YY, Wang X, Yang F, Wang LN, Wu DC (2018) Highly elastic and ultratough hybrid ionic-covalent hydrogels with tunable structures and mechanics. Adv Mater 30(18):e1707071
26. Fan HL, Wang JH, Jin ZX (2018) Tough, swelling-resistant, self-healing, and adhesive dual-cross-linked hydrogels based on polymer–tannic acid multiple hydrogen bonds. Macromolecules 51(5):1696–1705
27. Cipriano BH, Banik SJ, Sharma R, Rumore D, Hwang W, Briber RM, Raghavan SR (2014) Superabsorbent hydrogels that are robust and highly stretchable. Macromolecules 47(13):4445–4452
28. Cheng Y, Gray KM, David L, Royaud I, Payne GF, Rubloff GW (2012) Characterization of the cathodic electrodeposition of semi-crystalline chitosan hydrogel. Mater Lett 87:97–100
29. Rodrigues FHA, Fajardo AR, Pereira AGB, Ricardo NMPS, Feitosa JPA, Muniz EC (2012) Chitosan-graft-poly(acrylic acid)/rice husk ash based superabsorbent hydrogel composite: preparation and characterization. J Polym Res 19(12):1
30. Ladet SG, Tahiri K, Montembault AS, Domard AJ, Corvol MTM (2011) Multi-membrane chitosan hydrogels as chondrocytic cell bioreactors. Biomaterials 32(23):5354–5364
31. Treenate P, Monvisade P, Yamaguchi M (2014) Development of hydroxyethylacryl chitosan/alginate hydrogel films for biomedical application. J Polym Res 21(12):601
32. Kurdtabar M, Koutenaee RN, Bardajee GR (2018) Synthesis and characterization of a novel pH-responsive nanocomposite hydrogel based on chitosan for targeted drug release. J Polym Res 25(5):119
33. Wang T, Gunasekaran S (2006) State of water in chitosan–PVA hydrogel. J Appl Polym Sci 101(5):3227–3232
34. Zhang L, Zhao J, Zhu JT, He CC, Wang HL (2012) Anisotropic tough poly(vinyl alcohol) hydrogels. Soft Matter 8(40):10439–10447
35. Sun XX, Luo CH, Luo FL (2020) Preparation and properties of self-healable and conductive PVA-agar hydrogel with ultra-high mechanical strength. Eur Polym J (124):109465

36. He QY, Huang Y, Wang SY (2018) Hofmeister effect-assisted one step fabrication of ductile and strong gelatin hydrogels. Adv Funct Mater 28(5):1705069
37. Tobolsky AV, Carlson DW, Indictor N (1961) Rubber elasticity and chain configuration. J Polym Sci Polym Chem 54(159):175–192
38. Jiang GQ, Liu C, Liu XL, Chen QR, Zhang GH, Yang M, Liu FQ (2010) Network structure and compositional effects on tensile mechanical properties of hydrophobic association hydrogels with high mechanical strength. Polymer 51(6):1507–1515
39. Wang LY, Wang MJ (2016) Removal of heavy metal ions by poly(vinyl alcohol) and Carboxymethyl cellulose composite hydrogels prepared by a freeze–thaw method. ACS Sustain Chem Eng 4:2830–2837
40. Niknia N, Kadkhodaee R (2017) Factors affecting microstructure, physicochemical and textural properties of a novel gum tragacanth-PVA blend cryogel. Carbohydr Polym 155:475–482
41. Hu J, Kurokawa T, Hiwatashi K, Nakajima T, Wu ZL, Liang SM, Gong JP (2012) Structure optimization and mechanical model for microgel-reinforced hydrogels with high strength and toughness. Macromolecules 45:5218–5228
42. Jiang XC, Xiang NP, Zhang HX, Sun YJ, Lin Z, Hou LX (2018) Preparation and characterization of poly(vinyl alcohol)/sodium alginate hydrogel with high toughness and electric conductivity. Carbohydr Polym 186:377–383
43. Thanyacharoen T, Chuysinuanb P, Techasakul S, Nooeaid P, Ummartyotina S (2018) Development of a gallic acid-loaded chitosan and polyvinyl alcohol hydrogel composite: release characteristics and antioxidant activity. Int J Biol Macromol 107(Pt A):363–370
44. Fan LH, Yang H, Yang J, Peng M, Hu J (2016) Preparation and characterization of chitosan/gelatin/PVA hydrogel for wound dressings. Carbohydr Polym 146:427–434
45. Pretsch E, Bühlmann P, Badertscher M (2000) Structure determination of organic compounds. Springer-Verlag, Berlin
46. Flory PJ (1953) Principles of polymer chemistry. Cornell University Press, Ithaca
47. Wang L, Jian YK, Le XX, Lu W, Ma CX, Zhang JW, Huang YJ, Huang CF, Chen T (2018) Actuating and memorizing bilayer hydrogels for a self-deformed shape memory function. Chem Commun (Camb) 54(10):1229–1232
48. Lin P, Ma SH, Wang XL, Zhou F (2015) Molecularly engineered dual-crosslinked hydrogel with ultrahigh mechanical strength, toughness, and good self-recovery. Adv Mater 27(12):2054–2059
49. Bai RB, Yang JW, Suo ZG (2019) Fatigue of hydrogels. Eur J Mech A-Solid 74:337–370
50. Wang YJ, Zhang XN, Song YH, Zhao YP, Chen L, Su FM, Li LB, Wu ZL, Zheng Q (2019) Ultrastiff and tough Supramolecular hydrogels with a dense and robust hydrogen bond network. Chem Mater 31(4):1430–1440
51. Wang R, Wang Q, Li L (2003) Evaporation behaviour of water and its plasticizing effect in modified poly(vinyl alcohol) systems. Polym Int 52(12):1820–1826
52. Zhou XY, Zhao F, Guo YH, Rosenberger B, Yu GH (2019) Architecting highly hydratable polymer networks to tune the water state for solar water purification. Sci Adv 5:eaaw5484
53. Trieu HH, Qutubuddin S (1994) Polyvinyl alcohol hydrogels I. Microscopic structure by freeze-etching and critical point drying techniques. Colloid Polym Sci 272(3):301–309
54. Luo CH, Wei N, Sun XX, Luo FL (2020) Fabrication of self-healable, conductive, and ultra-strong hydrogel from polyvinyl alcohol and grape seed–extracted polymer. J Appl Polym Sci 137: e49118
55. Gurses MS, Erkey C, Kizilel S, Uzun A (2017) Characterization of sodium Tripolyphosphate and sodium citrate dehydrate residues on surfaces. Talanta 176:8
56. Kupiec TC, Goldenring JM, Vishnu R (2004) A non-fatal case of sodium toxicity. J Anal Toxicol 6:6